

Role of nematicity in controlling spin fluctuations and superconducting T_c in bulk FeSe

Swagata Acharya, Dimitar Pashov, and Mark van Schilfgaarde

*King's College London, Theory and Simulation of Condensed Matter, The Strand, WC2R 2LS London, UK**

Bulk FeSe superconducts inside a nematic phase, that sets in through an orthorhombic distortion of the high temperature tetragonal phase. Bulk non-alloy tetragonal superconducting FeSe does not exist as yet. This raises the question whether nematicity is fundamental to superconductivity. We employ an advanced ab-initio ability and show that bulk tetragonal FeSe can, in principle, superconduct at almost the same T_c as the orthorhombic phase had that been the ground state. Further, we perform rigorous benchmarking of our theoretical spin susceptibilities against experimentally observed data over all energies and relevant momentum direction. We show that susceptibilities computed in both the tetragonal and orthorhombic phases already have the correct momentum structure at all energies, but not the desired intensity. The enhanced nematicity that simulates the correct spin fluctuation intensity can only lead to a maximum 10-15% increment in the superconducting T_c . Our results suggest while nematicity may be intrinsic property of the bulk FeSe, is not the primary force driving the superconducting pairing.

Bulk FeSe superconducts below 9 K, deep inside an orthorhombic phase that sets in at a much higher temperature 90 K¹. The normal bulk tetragonal phase does not superconduct unless it is doped²⁻⁶ or forms a monolayer^{7,8}. A non-alloy bulk tetragonal superconducting FeSe does not exist just yet. This raises the question if the nematicity facilitates superconductivity in the bulk or not⁹⁻¹¹. Further recent studies have suggested that there exists strong spin fluctuation anisotropy possibly originating from electronic nematicity inside the d-twinned orthorhombic phase¹². This enhanced electronic anisotropy shows up in the inelastic neutron scattering (INS), in resistivity measurements¹³, in angle resolved photo-emission spectroscopic studies¹⁴⁻¹⁶ and in several other measurements¹⁷. How such spin fluctuations affect the superconducting instability is a subject of intensive study presently.

In this letter, we take a systematic approach towards studying the spin fluctuations inside the tetragonal and orthorhombic phases of bulk FeSe, and we probe the role of nematicity on spin fluctuations and superconductivity. We perform rigorous benchmarking against existing susceptibility data from INS measurements¹⁸. We show that spin susceptibilities are nearly indistinguishable for the two phases. Further, we split the crystalline planar rotational symmetry by an enhanced factor and show the the resulting anisotropy simulates the best possible agreement against the existing INS data inside the orthorhombic phase. While this enhanced structural nematicity is not physical, it is an approximate way to mimic the nematicity by adding anisotropy to the potential through the external potential rather than through nonlocal spin fluctuations. The effect is similar : it enhances nematicity that, as we show, generates a spin susceptibility that replicates neutron measurements. We can then assess its impact on superconductivity, since spin fluctuations are the primary driving force for superconductivity, and we find that this enhanced nematicity has only very moderate effect.

We are able to make these findings thanks to recent developments that couple (quasi-particle) self consistent GW (QSGW) with dynamical mean field theory (DMFT)¹⁹⁻²². Merging these two state-of-the-art methods captures the effect of both strong local dynamic spin fluctuations (captured well in DMFT), and non-local dynamic correlation^{23,24} effects captured by QSGW²⁵. On top of the DMFT self-energy, charge and spin susceptibilities are obtained from vertex functions computed from the two-particle Green's function generated in DMFT, via the solutions of non-local Bethe Salpeter equation (BSE). Additionally, we compute the particle-particle vertex functions and solve the linearized Eliashberg equation^{21,26,27} to compute the superconducting susceptibilities and eigenvalues of superconducting gap instabilities.

In Fig. 1 we plot the imaginary part of the dynamic and momentum resolved spin susceptibilities $\text{Im}\chi(q, \omega)$ (tetragonal and nematic) and compare them against the inelastic neutron scattering (INS) data received from Wang et al.¹⁸. $\text{Im}\chi(q, \omega)$ plotted at $\omega = 15, 35, 40$ and 80 meV along the path $\mathbf{Q}=(1, \text{K})$ at $L=0$ in reciprocal lattice units of one Fe-atom unit cell. The structural orthorhombic distortion ($a=5.3100 \text{ \AA}$, $b=5.3344 \text{ \AA}$) that sets in around 90 K is fairly weak (in the tetragonal phase $a=3.779 \text{ \AA}$, $\sqrt{2}a=5.3443 \text{ \AA}$). Consequently, $\text{Im}\chi(q, \omega)$ remains nearly invariant in the tetragonal and orthorhombic phases over all energies and momentum. Most remarkably, we reproduce the entire momentum dependence structure of $\text{Im}\chi(q, \omega)$ at all energies in both the phases. This is a testimony to the fact that the essential elements that are required to produce the momentum and energy structures for $\text{Im}\chi(q, \omega)$ are already present in our three tier QSGW+DMFT+BSE approximation. Nevertheless, our computed $\text{Im}\chi(q, \omega)$ remains smaller than the experimental results around $\mathbf{Q}=(1, 1)$ at all energies.

One of the reasons for this discrepancy could be the absence of electronic nematicity from the approxima-

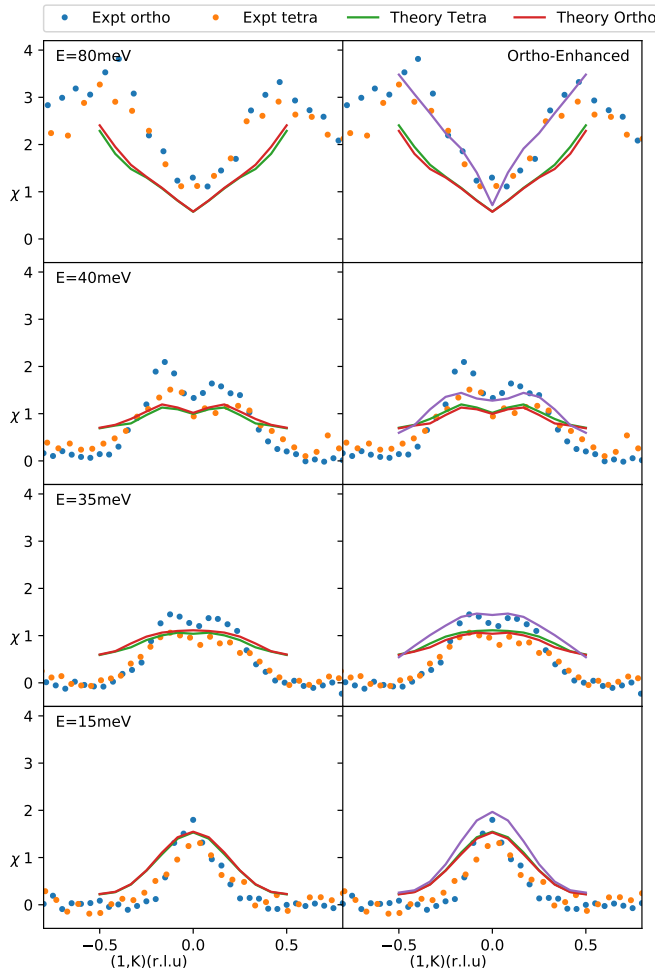


FIG. 1. Imaginary part of the dynamic spin susceptibility $\text{Im}\chi(q, \omega)$ plotted along the path $\mathbf{Q}=(1, K)$ at $L=0$ in reciprocal lattice units of one Fe-atom unit cell. Different energy cuts are taken and plotted against the observed $\text{Im}\chi(q, \omega)$ in inelastic Neutron scattering (INS) experiment¹⁸. The experimental data is reproduced with the raw data received from Wang et al. We plot our computed $\text{Im}\chi(q, \omega)$ at $\omega=15, 35, 40$ and 80 meV against INS data. Theoretically, the data for the tetragonal (green continuous line) and orthorhombic (red continuous line) phases are nearly indistinguishable and both of them deviate from the experimental data (the latter is plotted as orange (tetra) and blue (ortho) circular points). The theoretical data for the enhanced orthorhombic distortion (purple continuous line) remarkably agrees with the experimental INS data for all energies and momentum.

tions that are involved in solving the QSGW+DMFT Hamiltonian. Electronic nematicity can only be incorporated in presence of momentum dependent self energy and vertex corrections which are longer range in nature, beyond the approximation of single site DMFT. At present we do not have the ability to incorporate such longer range electronic fluctuations *ab initio*. We instead nematicity by modifying the crystal-field splitting, enlarging the orthorhombic splitting by a factor of five to ($a=5.3100$ Å, $b=5.4344$ Å). In the rest of the paper we

use ‘ortho-enhanced’ to identify this particular structure. We find that the resulting $\text{Im}\chi(q, \omega)$ is enhanced in intensity and produces remarkable agreement with the INS data over all energies and momentum. This is crucial, since it is thought that in bulk FeSe spin fluctuations are the primary source of superconductivity. While the source of the potential driving this nematicity is artificial, it appears, the anisotropy in potential is similar to the anisotropy that would derive from the nonlocal contribution to the self-energy from spin fluctuations. This warrants a more rigorous investigation of this ortho-enhanced electronic structure.

First, we study the effects of these different crystalline geometry on the local density of states (DOS) of the systems. We plot the QSGW+DMFT DOS for the three systems; tetragonal, orthorhombic and ortho-enhanced. Note that the QSGW Green’s functions are renormalized in the presence of the self-consistent single-site DMFT self energy. We observe that for all phase there is a significant dip in the density of states around Fermi energy. However, while this ortho-enhanced set up is observed to produce detectable changes to the intensity of $\text{Im}\chi(q, \omega)$ over all energies and momentum, its effect of the local DOS is fairly weak. We observe a weak suppression of the DOS at and around $\omega=0$ (see Fig. 2). However, this observation suggests that photo-emission spectroscopic methods should be able to see this drop in the local DOS at low energies in systems where nematicity plays a major role, for example, in the de-twinning sample of FeSe^{12,15,28}. It suggests that if the superconductivity is modified by enhanced nematicity, it does not result from a purely Fermi surface nesting driven mechanism; rather, the change in two-particle vertex associated with such fluctuations has to promote the superconducting pairing glue.

Before exploring superconductivity, we study the DMFT spectral functions $A(k, \omega)$. We plot $A(\omega)$ for selected values of k on the M- Γ and A-Z lines. Fig. 2 shows how the electron pockets evolve into hole pockets along those paths. We find that the enhanced nematicity leads to weak changes in the hole pockets: while at $A(\Gamma, \omega)$ decreases, but $A(Z, \omega)$ increases and splits (see Fig. 2). Moreover, close to M and A points, $A(\omega)$ is weakly suppressed and slightly broadened.

We study next, how these affect the real part of the spin susceptibilities $\chi(q, \omega=0)$. We resolve our computed static spin susceptibilities $\chi(q)$ in different intra-orbital channels. We observe that the $\chi(q)$ increases in all intra-orbital channels due to the enhanced nematicity, however, $\chi(q)$ remains smaller in the d_{xz} and d_{yz} channels in comparison to the d_{xy} channel (see Fig. 3). Orthorhombic distortion lifts the degeneracy between the d_{xz} and d_{yz} orbitals. Enhanced orthorhombic distortion in case of ortho-enhanced further magnifies this splitting. In the detwinned sample of FeSe, with one Fe atom cell, it is observed that the spin susceptibility peaks at $\mathbf{Q}=(1, 0)$ and $(0, 1)$ become significantly different¹². This raises the question whether nematicity play an important role

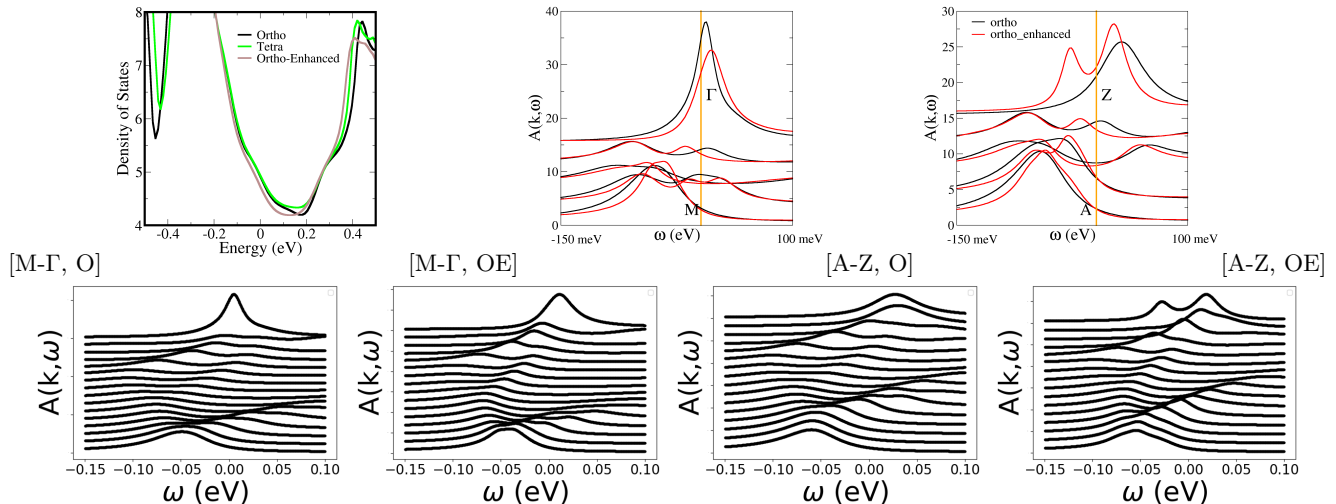


FIG. 2. The total local density of states (DOS) for FeSe in tetragonal, orthorhombic (O) and orthorhombic phase with enhanced distortion (OE) are shown. In the bottom panels $A(\omega)$ is plotted for a sequence of k on the M- Γ and A-Z lines. Top right panels superpose O and OE spectral functions for a few values of k to bring out the effects of the nematicity.

in formation of Cooper pairing as well. While our theory can not address the problem in detwinned FeSe, we show that the enhanced structural nematicity that we simulate through ortho-enhanced structure leads to weak changes in $\text{Re}\chi(q)$ at $\omega=0$ in the bulk two-atom unit cell of FeSe in comparison to the tetragonal and orthorhombic phases. However, as we showed before in Fig. 1, orthorhombic distortion must be artificially enhanced to produce the excellent agreement against the experimentally observed $\text{Im}\chi(q, \omega)$ in the same bulk phase. Taken together, this suggests that a small degree of nematicity originates from the external potential, but most of it originates from non-local many-body spin fluctuations. In any case the d_{xy} channel remains the dominant spin fluctuation channel, while the d_{xz} and d_{yz} channels each contribute nearly 40% of the d_{xy} spin fluctuations.

How particular orbitals govern spin fluctuations and thus control T_c , is key to understanding the superconducting mechanism in such a complex multi-band manifold. We probe the effect of such enhanced nematicity on the superconductivity. We solve the superconducting gap equations within the BCS approximation^{26,29}, which includes the full momentum and orbital dependence in the vertex functions, but is taken to be static in the two Fermionic frequencies. With the full frequency dependent vertex, the rank of Eliashberg matrix for a five orbital problem is in excess of 1 million. For detailed description see Ref²⁹ and the supplemental material therein. BCS, which approximates the vertex as static, is a reasonable approximation, as superconductivity is essentially a low energy phenomenon.

We observe that the leading eigenvalue of the superconducting gap equation corresponds to an extended s-wave gap structure³⁰, with a form factor $\Delta_1 \sim \cos(k_x) - \cos(k_y)$ 4

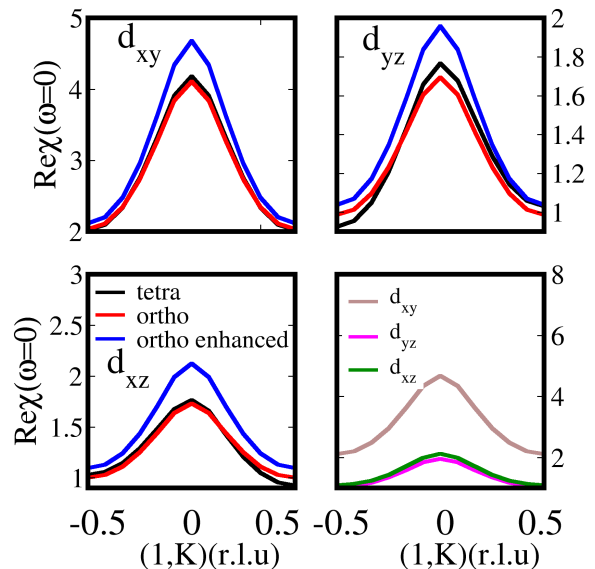


FIG. 3. Static spin susceptibility, $\text{Re}\chi(q)$ is orbitally resolved and plotted along $\mathbf{Q}=(1,K)$ at $L=0$ in reciprocal lattice units of one Fe-atom unit cell. The enhanced orthorhombic distortion increases the intensity of $\text{Re}\chi(q)$ in all intra-orbital channels, however, the d_{xy} states remain dominant in all cases.

in all the phases (and the lagging instability Δ_2 has a $\cos(k_x) + \cos(k_y)$ structure). Moreover, this dominant instability exists in the d_{xy} orbital channel, consistent with our observations of dominant spin fluctuations in the same channel. We also observe, intriguingly, that

the orthorhombic distortion weakly suppresses the bubble (χ^0) contribution to the pairing and the strength of the interaction vertex Γ remains nearly unchanged from the tetragonal phase, and hence, the pairing susceptibility ($\sim \Gamma \times \chi^0$) gets weakly suppressed. However, in ortho-enhanced, the Γ is significantly enhanced and the χ^0 drops (directly related to our observation of weak suppression in $A(k, \omega=0)$). The increment in Γ overcompensates for the loss in the χ^0 and the net $\Gamma \times \chi^0$ still enhances in comparison to the tetragonal phase. Our calculations suggest that the net effect is to increase the eigenvalue corresponding to the leading superconducting instability and thereby this enhanced nematicity potentially can drive a higher T_c . Where the leading eigenvalue reaches one, is the T_c . As we showed in our recent work²⁹ that it is extremely challenging to perform the calculations at a low enough temperature where λ can become unity, due to several technicalities primarily related to the stochastic nature of the CT-QMC solver. The lowest temperature where could perform our calculations in these systems is 116 K, and the λ is not unity. However, following the trend, it appears that the ortho-enhanced phase can at most realize a 10-15% enhancement in T_c in comparison to the bulk orthorhombic phase. However, our calculations suggest that the tetragonal phase could also superconduct with a T_c not much different from the ortho-enhanced phase. This is consistent with the experimental observation that the $\text{FeSe}_{1-x}\text{S}_x$ alloy realizes a superconducting T_c not significantly different from the bulk orthorhombic FeSe, even when sulphur doping suppresses the nematic phase completely³¹⁻³³.

To summarize, we perform *ab initio* calculations for bulk tetragonal and orthorhombic phases of FeSe and compute single and two-particle spectra and superconducting eigenvalues. We find that the spin fluctuations are dominant in the Fe-3d_{xy} channel in all cases and can potentially drive superconductivity in the bulk tetragonal FeSe. Nevertheless, a rigorous comparison against the observed spin susceptibilities in inelastic neutron scattering experiments in the orthorhombic phase reveals that our computed susceptibilities have the correct momentum structure at all energies, but not the intensity. We show that an artificially enhanced structural orthorhombic distortion simulates the missing spin fluctuation intensity and acts as the proxy for the, most likely, electronic nematicity, missing from our theory but present in the real world. This enhanced nematicity, however, at

best can account for an 10-15% increment in T_c .

ACKNOWLEDGMENTS

We acknowledge Qisi Wang and Jun Zhao for sharing with us the raw data for spin susceptibilities. This work was supported by the Simons Many-Electron Collaboration. We acknowledge PRACE for awarding us access to SuperMUC at GCS@LRZ, Germany, STFC Scientific Computing Department's SCARF clus-

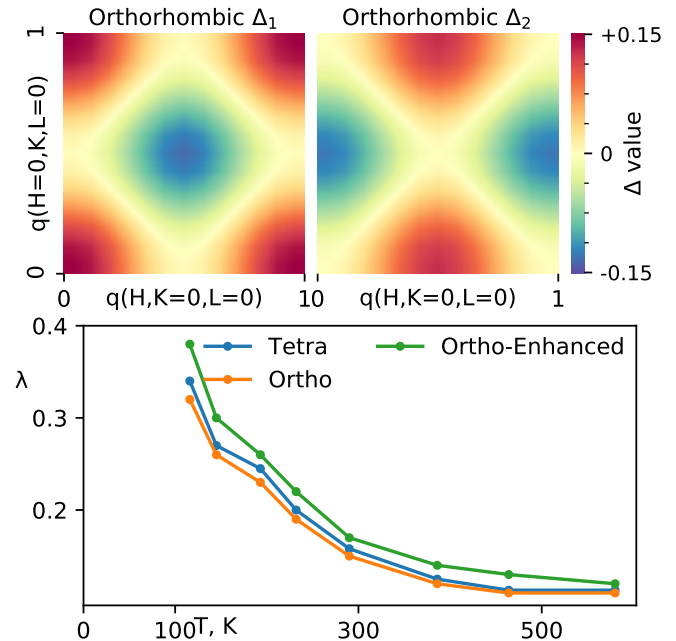


FIG. 4. The superconducting instabilities inside the orthorhombic phase are shown: instabilities correspond to the leading (Δ_1) and lagging (Δ_2) eigenvalues of the solutions to the BCS gap equation. The evolution of the leading eigenvalue as a function of temperature is shown for tetragonal, orthorhombic and ortho-enhanced phases in the bottom panel.

ter, Cambridge Tier-2 system operated by the University of Cambridge Research Computing Service (www.hpc.cam.ac.uk) funded by EPSRC Tier-2 capital grant EP/P020259/1.

* swagata.acharya@kcl.ac.uk

¹ T. M. McQueen, A. J. Williams, P. W. Stephens, J. Tao, Y. Zhu, V. Ksenofontov, F. Casper, C. Felser, and R. J. Cava, *Phys. Rev. Lett.* **103**, 057002 (2009).

² Y. Mizuguchi, F. Tomioka, S. Tsuda, T. Yamaguchi, and Y. Takano, *Applied Physics Letters* **93**, 152505 (2008).

³ R. Shipra, H. Takeya, K. Hirata, and A. Sundaresan, *Physica C: Superconductivity* **470**, 528 (2010).

⁴ A. Galluzzi, M. Polichetti, K. Buchkov, E. Nazarova, D. Mancusi, and S. Pace, *Superconductor Science and Technology* **30**, 025013 (2016).

⁵ F. Sun, Z. Guo, H. Zhang, and W. Yuan, *Journal of Alloys and Compounds* **700**, 43 (2017).

⁶ L. Craco, M. Laad, and S. Leoni, in *Journal of Physics: Conference Series*, Vol. 487 (IOP Publishing, 2014) p. 012017.

- ⁷ W. Qing-Yan, L. Zhi, Z. Wen-Hao, Z. Zuo-Cheng, Z. Jin-Song, L. Wei, D. Hao, O. Yun-Bo, D. Peng, C. Kai, *et al.*, Chinese Physics Letters **29**, 037402 (2012).
- ⁸ J.-F. Ge, Z.-L. Liu, C. Liu, C.-L. Gao, D. Qian, Q.-K. Xue, Y. Liu, and J.-F. Jia, Nature materials **14**, 285 (2015).
- ⁹ A. E. Böhmer and A. Kreisel, Journal of Physics: Condensed Matter **30**, 023001 (2017).
- ¹⁰ A. V. Chubukov, M. Khodas, and R. M. Fernandes, Physical Review X **6**, 041045 (2016).
- ¹¹ Q. Wang, Y. Shen, B. Pan, Y. Hao, M. Ma, F. Zhou, P. Steffens, K. Schmalzl, T. Forrest, M. Abdel-Hafiez, *et al.*, Nature materials **15**, 159 (2016).
- ¹² T. Chen, Y. Chen, A. Kreisel, X. Lu, A. Schneidewind, Y. Qiu, J. Park, T. G. Perring, J. R. Stewart, H. Cao, *et al.*, Nature materials **18**, 709 (2019).
- ¹³ M. A. Tanatar, A. E. Böhmer, E. I. Timmons, M. Schütt, G. Drachuck, V. Taufour, K. Kothapalli, A. Kreyssig, S. L. Budko, P. C. Canfield, *et al.*, Physical review letters **117**, 127001 (2016).
- ¹⁴ M. Watson, T. Kim, L. Rhodes, M. Eschrig, M. Hoesch, A. Haghighirad, and A. Coldea, Physical Review B **94**, 201107 (2016).
- ¹⁵ M. D. Watson, A. A. Haghighirad, L. C. Rhodes, M. Hoesch, and T. K. Kim, New Journal of Physics **19**, 103021 (2017).
- ¹⁶ A. I. Coldea and M. D. Watson, Annual Review of Condensed Matter Physics **9**, 125 (2018).
- ¹⁷ A. Böhmer, T. Arai, F. Hardy, T. Hattori, T. Iye, T. Wolf, H. v. Löhneysen, K. Ishida, and C. Meingast, Physical review letters **114**, 027001 (2015).
- ¹⁸ Q. Wang, Y. Shen, B. Pan, X. Zhang, K. Ikeuchi, K. Iida, A. Christianson, H. Walker, D. Adroja, M. Abdel-Hafiez, *et al.*, Nature communications **7**, 1 (2016).
- ¹⁹ L. Sponza, P. Pisanti, A. Vishina, D. Pashov, C. Weber, M. van Schilfhaarde, S. Acharya, J. Vidal, and G. Kotliar, Phys. Rev. B **95**, 041112 (2017).
- ²⁰ S. Acharya, D. Dey, T. Maitra, and A. Taraphder, Journal of Physics Communications **2**, 075004 (2018).
- ²¹ S. Acharya, D. Pashov, C. Weber, H. Park, L. Sponza, and M. Van Schilfhaarde, Communications Physics **2**, 1 (2019).
- ²² E. Baldini, M. A. Sentef, S. Acharya, T. Brumme, E. Sheveleva, F. Lyzwa, E. Pomjakushina, C. Bernhard, M. van Schilfhaarde, F. Carbone, A. Rubio, and C. Weber, Proceedings of the National Academy of Sciences (2020), 10.1073/pnas.1919451117, <https://www.pnas.org/content/early/2020/03/10/1919451117.full.pdf>.
- ²³ J. Tomczak, P. Liu, A. Toschi, G. Kresse, and K. Held, The European Physical Journal Special Topics **226**, 2565 (2017).
- ²⁴ D. Pashov, S. Acharya, W. R. Lambrecht, J. Jackson, K. D. Belashchenko, A. Chantis, F. Jamet, and M. van Schilfhaarde, Computer Physics Communications **249**, 107065 (2020).
- ²⁵ T. Kotani, M. van Schilfhaarde, and S. V. Faleev, Phys. Rev. B **76**, 165106 (2007).
- ²⁶ H. Park, *The study of two-particle response functions in strongly correlated electron systems within the dynamical mean field theory*, Ph.D. thesis, Rutgers University-Graduate School-New Brunswick (2011).
- ²⁷ Z. Yin, K. Haule, and G. Kotliar, Nature Physics **10**, 845 (2014).
- ²⁸ L. C. Rhodes, M. D. Watson, A. A. Haghighirad, D. V. Evtushinsky, and T. K. Kim, arXiv preprint [arXiv:2004.04660](https://arxiv.org/abs/2004.04660) (2020).
- ²⁹ S. Acharya, D. Pashov, F. Jamet, and M. van Schilfhaarde, arXiv preprint [arXiv:2003.13156](https://arxiv.org/abs/2003.13156) (2020).
- ³⁰ B. Zeng, G. Mu, H. Luo, T. Xiang, I. Mazin, H. Yang, L. Shan, C. Ren, P. Dai, and H.-H. Wen, Nature communications **1**, 112 (2010).
- ³¹ K. Matsuura, Y. Mizukami, Y. Arai, Y. Sugimura, N. Maejima, A. Machida, T. Watanuki, T. Fukuda, T. Yajima, Z. Hiroi, *et al.*, Nature communications **8**, 1 (2017).
- ³² S. Hosoi, K. Matsuura, K. Ishida, H. Wang, Y. Mizukami, T. Watashige, S. Kasahara, Y. Matsuda, and T. Shibauchi, Proceedings of the National Academy of Sciences **113**, 8139 (2016).
- ³³ P. Reiss, D. Graf, A. A. Haghighirad, W. Knafo, L. Drigo, M. Bristow, A. J. Schofield, and A. I. Coldea, Nature Physics **16**, 89 (2020).